

A NEW HEAT BALANCE FOR FLOW BOILING

Francisco J. Collado*, Carlos Monné*, Antonio Pascau[‡]

*Dpto. Ingeniería Mecánica, CPS-B, [‡]Dpto. Ciencia Materiales&Fluidos, CPS-C
Univ. Zaragoza, Zaragoza, 50018, Spain

Phone: +34 976 762551, Fax: +34 976 762616, E-mail: fjk@unizar.es

Abstract

Recently, one of the authors suggested calculating void fraction, an essential element in thermal-hydraulics, working with the 'thermodynamic' quality instead of the usual 'flow' quality. However, the standard heat balance is currently stated as a function of the 'flow' quality. Therefore, we should search a new energy balance between the mixture enthalpy, based on 'thermodynamic' quality, and the absorbed heat. This work presents the results of such analysis based on accurate measurements of the axial profile of the cross-sectional average void fraction in the region of boiling with subcooling for water at medium and high pressures taken by Moscow Power Institute (MPI) and Argonne National Laboratory (ANL). As main results, we find that, under uniform heat flux, the mixture enthalpy suffers an abrupt reduction of its slope in passing saturation, and a new slip ratio could balance heat with such mixture enthalpy.

Keywords: flow boiling, void fraction, slip ratio, heat balance, mixture enthalpy

1. Introduction

A large number of correlations [1-6] have been proposed for the evaluation of the cross-sectional average volumetric fraction or void fraction of vapor bubbles, α , which is of considerable interest to power and process industries because void fraction significantly affects neutron absorption, heat transfer and pressure drop [1-6]. Unfortunately, the non-equilibrium complexities in the subcooled region, in which saturated vapor bubbles steadily co-exist with subcooled bulk liquid, have prevented to define a coherent expression of the heat balance for subcooled flow boiling [1-6].

So, for void fraction calculation, the standard expression for the heat balance for this zone, and the full boiling region, is the definition of an 'equilibrium' quality [1-6] x_{eq} as

$$\underbrace{x_{eq}h_G + (1 - x_{eq})h_F}_{h_{flow}} = q'z + h_{L,i} \Rightarrow x_{eq} = (q'z + h_{L,i} - h_F) / (h_G - h_F), \quad (1)$$

where q' is the uniform heat per unit length and per unit inlet mass (kJ/m-kg), z is the axial distance along the heated wall (m), $h_{L,i}$ is the inlet liquid enthalpy (assuming only liquid at the inlet) (kJ/kg), and h_F and h_G are the saturated liquid and saturated vapor enthalpies at the inlet pressure, respectively (kJ/kg). Usually, the kinetic and gravity terms are neglected [1-6].

It is clear from Eq. (1) that this quality will take negative values along the subcooled zone i.e., until liquid reaches saturation ($x_{eq} = 0$). Evidently, a negative quality has no physical sense and it should be merely taken as a good indicator of the relative thermal distance of the subcooled liquid to saturation. After saturation, the above quality now is positive, being also called 'flow' quality, x_{flow} .

To relate this 'equilibrium' quality with the unknown true local vapor weight fraction, Levy in [4] postulated an exponential function. Recently, Delhay et al. in [5] have postulated a hyperbolic tangent function. Then, the vapor volumetric fraction is obtained from this true local vapor weight fraction and accepted relationships between vapor weight and volumetric fractions, which were based mainly on the 'drift flux' model of Zuber and Findlay [6], see also [5]. The 'drift flux' model is complex and empirical [5-6], including some particular shape for the transverse or radial void fraction profile through a distribution parameter, and treating the physical fact that the velocities of the vapor and the liquid are different defining the so-called 'weighted drift' velocity [5-6]. The distribution parameter and the 'weighted drift' velocity are always determined from experimental database.

Classically, the difference of velocities between the phases has been alternatively quantified through the slip ratio S [1-3], which is defined as the cross-sectional area mean vapor velocity c_G (m/s) divided by the cross-sectional area mean liquid velocity c_L (m/s). Its standard expression [1-3] in function of 'flow' quality x_{flow} (so S would be a 'flow' slip), void fraction α and saturated liquid and vapor densities ρ_F and ρ_G , respectively is

$$S_{flow} = c_G/c_L = [x_{flow}(1-\alpha)\rho_F] / [(1-x_{flow})\alpha\rho_G]. \quad (2)$$

In conclusion, due to the strong difficulties of treating subcooled flow boiling, the standard procedures to calculate the void fraction are necessarily rather complex and empirical. Furthermore, there is a lack of a general heat balance expression which were valid from subcooling to boiling, and there is no physical justification for an 'equilibrium' quality with negative values along subcooling, which would also imply negative values of the classic slip ratio, see Eq. (2), again without explanation.

The main novelty of this work is to use classic thermodynamic relationships between vapor weight and volumetric fractions i.e., to deal with the well-known 'thermodynamic' quality x_{th} , classically defined as [3]

$$x_{th} = \rho_G \alpha / \rho_m, \quad (3)$$

where ρ_m is the standard mixture density of the vapor-liquid mixture (kg/m^3). This was first suggested by Bilicki et al. [7-8], who pointed out that if we are able to accurately measure the void fraction α –indeed, the mixture density- by gamma-ray or X-ray attenuation, its corresponding actual mass fraction -following classical Thermodynamics- would be the thermodynamic quality x_{th} , and not the 'flow' quality x_{flow} .

In a recent work [9], we have already analyzed the evident thermodynamic relation between the measured void fraction and the ‘thermodynamic’ quality. Briefly, it can be easily shown that x_{th} would be the true vapor weight fraction, merely using the specific volume of the mixture. So that, we first state the standard mixture density [1-3]

$$\rho_m = \alpha\rho_G + (1 - \alpha)\rho_L, \quad (4)$$

where ρ_L is the density of the liquid (kg/m³), which might be subcooled or saturated. Now the inverse of the mixture density is the mixture specific volume, v_m . Then, if we write v_m as a combination of the liquid (saturated or subcooled) and vapor specific volumes weighted by the actual vapor mass fraction of the mixture x' , whatever it be, we readily arrive to the result that this actual vapor mass fraction coincides with the ‘thermodynamic’ quality stated in Eq. (3)

$$v_m = x'v_G + (1 - x')v_L = x'/\rho_G + (1 - x')/\rho_L = 1/\rho_m \quad \Rightarrow \quad x' = x_{th} = \alpha\rho_G/\rho_m. \quad (5)$$

Finally, the derivation of α in function of x_{th} and the densities of the phases is immediate from Eqs. (3)-(4)

$$\alpha = x_{th}(\rho_L/\rho_G)/[x_{th}(\rho_L/\rho_G) + (1 - x_{th})]. \quad (6)$$

Now the key question would be how the applied heat can be related with the mixture enthalpy increment Δh_m , which here is also based on the ‘thermodynamic’ quality x_{th}

$$h_m = x_{th}h_G + (1 - x_{th})h_L \quad \Rightarrow \quad \Delta h_m = h_m - h_{L,i}. \quad (7)$$

So that, we should compare the axial profile of such ‘thermodynamic’ mixture enthalpy of the fluid, passing through a uniform heated duct, with the heat input per unit mass. However, previous works [9-10] have shown that there are strong discrepancies between this mixture enthalpy and heat. Although, it has been also found [9-10] that the explicit inclusion of the slip ratio could close the balance between the absorbed heat and the mixture enthalpy increment.

Therefore, here we will check the following relation, which explicitly includes a new slip ratio

$$q'z/S_{new} \sim h_m(z) \quad (8)$$

For this comparison, we will use two independent data sets, both with uniform heat flux applied along the duct. First, the accurate measurements of the axial profile of the cross-sectional average void fraction in the region of boiling with subcooling, taken by the Moscow Power Institute in the seventies, for flow boiling of water at high pressure in vertical, upwards, round tubes. In particular, the 24 tests reported by Bartolomei et al. in [11], in which the pressure, mass fluxes and heat fluxes ranged from 3.01 MPa to 14.68 MPa, from 405 to 2123 kg m⁻² s⁻¹ and from 0.42 to 2.21 MWm⁻², respectively.

And second, some of the tabulated data from one series of investigations of the density of steam-water mixtures carried out by Argonne National Laboratory (ANL) in the sixties and reported by Marchaterre et al. in [12]. These data were taken for natural and forced circulation in rectangular, vertical, upwards channels over a velocity range of 0.31-1.8 m/s, a flow quality range of 0 to 6 %, and a pressure range of 1.13- 4.14 MPa.

As major results of this analysis, we find that, under uniform heat flux, the thermodynamic mixture enthalpy suffers an abrupt reduction of its slope in reaching saturation. This change of slope is logically related with the well-known change of curvature of the measured axial profile of void fraction at saturation. Furthermore, a new slip ratio could close the balance between heat and mixture enthalpy. However, there is a strong relation between the new slip ratio and the standard one.

In conclusion, it would be possible an accurate prediction of the void fraction axial profile through the mixture enthalpy, see Eqs. (6)-(7), derived from the new heat balance. So that it would be necessary to know only three parameters for each test. The first one would be the beginning of the subcooled boiling region, classically defined as the point of net vapor generation (PNVG) [13-14], which in this work will be identified as a PNVG 'equilibrium' quality $x_{eq-PNVG}$. The other two ones would be particular values of the new slip ratio namely, the slip ratio at the end of the subcooling region i.e., just at saturation, and the average of the new slip ratio along full boiling.

2. MPI Measurements of the Axial Profile of Void fraction

Hundreds of accurate measurements of the axial profile of the void fraction in the region of boiling with subcooling for water at high pressure were carried out in the seventies at the Moscow Power Institute (MPI) for a wide range of severe operating conditions. Bartolomei et al. presented in [11] only some samples to show the main trends about the influence of heat flux, mass velocity and pressure on void fraction. In the 24 tests reported in [11], the inlet pressure p_i , mass flux G and heat flux q'' range from 3.01 MPa to 14.68 MPa, from 405 to 2123 kg m⁻² s⁻¹ and from 0.42 to 2.21 MWm⁻², respectively.

A closed loop rig allowed measure inlet pressure (MPa), inlet temperature (°C), mass velocity (kg/s-m²) and uniform heat flux release (MW/m²) over the length of vertical channels, while the motion of the medium was upwards. The experimental channels were made up of commercial tubes 12·10⁻³ m of internal diameter and 2·10⁻³ m of wall thickness, with heated lengths from 0.8 to 1.5 m. Maximum relative errors within the entire range of investigations did not exceed 0.01 for pressure, 0.02 for mass velocity and 0.03 for heat flux density. The maximum absolute error of temperature measurement did not exceed 1 K.

The main investigated parameter was true volumetric steam content α . It was determined by penetrating γ -radiation from a Tu-170 source. Measurement was carried out with a wide diverging pencil covering the passage cross-section and part of the channel wall to make up channel expansions. Although the accuracy of a determination by this procedure is governed by many factors, maximum absolute errors within the investigated range of parameters did not exceed ± 0.04 .

In Table 1, the characteristics of the 24 MPI tests are shown. They have been gathered and named following the number of the figures and the increase of the operational parameter (O. P.) varied [11]. The shaded tests, although repeated, are included to analyze the influence of heat flux, mass velocity and pressure in the model.

Table 1. Conditions of the tests presented by Bartolomei et al. in [11]

O. P. varied	# Test	p_i (MPa)	G (kg/m ² s)	q'' (MW/m ²)	$\Delta T_{sub,i}$ (° C)	$c_{L,i}$ (m/s)	$x_{eq-PNVG}$	$S_{1,sat}$	S_2	$\alpha_{o,mea}$	$\alpha_{o,cal}$
none	1-1	6.89	985	1.13	93.9	1.12	-0.1	0.936	2.99	0.490	0.486
	1-2	6.78	1071	1.13	91.8	1.22	-0.13	0.921	2.19	0.538	0.523
	1-3	6.84	961	1.13	91.4	1.10	-0.12	0.927	2.29	0.590	0.587
	1-4	6.84	995	1.15	91.4	1.13	-0.10	0.927	2.48	0.585	0.556
q''	2a-1	6.81	998	0.44	36.1	1.24	-0.05	0.93	2.17	0.296	0.297
	2a-2	6.89	965	0.78	64.9	1.14	-0.08	0.905	2.29	0.488	0.487
	2a-3	6.84	961	1.13	91.4	1.10	-0.12	0.927	2.29	0.590	0.587
	2a-4	6.74	988	1.7	140.4	1.07	-0.13	0.938	2.41	0.575	0.573
	2a-5	7.01	996	1.98	125.1	1.09	-0.15	0.935	3.34	0.463	0.458
q''	2b-1	14.79	1878	0.42	11.2	2.89	-0.03	0.906	(3.74)	0.067	0.087
	2b-2	14.74	1847	0.77	15.9	2.78	-0.1	0.900	1.35	0.350	0.348
	2b-3	14.75	2123	1.13	31.0	3.02	-0.12	0.891	1.35	0.288	0.289
	2b-4	14.70	2014	1.72	68.7	2.59	-0.12	0.911	(4.4)	0.216	0.216
	2b-5	14.99	2012	2.21	52.3	2.70	-0.18	0.863	-	0.185	0.185
G	3a-1	6.89	405	0.79	136.9	0.44	-0.14	0.925	2.56	0.600	0.598
	3a-2	6.89	965	0.78	64.9	1.14	-0.08	0.905	2.29	0.488	0.487
	3a-3	6.89	1467	0.77	38.9	1.81	-0.09	0.909	-	0.175	0.173
	3a-4	6.79	2024	0.78	36.9	2.51	-0.04	0.900	-	0.225	0.225
G	3b-1	11.02	503	0.99	97.4	0.59	-0.19	0.910	1.69	0.550	0.540
	3b-2	10.81	966	1.13	87.9	1.16	-0.15	0.906	1.99	0.490	0.498
	3b-3	10.81	1554	1.16	26.9	2.1	-0.12	0.795	1.70	0.488	0.489
	3b-4	10.84	1959	1.13	27.1	2.65	-0.07	0.875	1.40	0.508	0.518
p _i	4a-1	3.01	990	0.98	62.2	1.1	-0.06	0.960	2.86	0.49	0.490
	4a-2	4.41	994	0.90	66.4	1.13	-0.09	0.930	2.74	0.586	0.570
	4a-3	6.84	961	1.13	91.4	1.10	-0.12	0.927	2.29	0.59	0.587
	4a-4	10.81	966	1.13	87.9	1.16	-0.15	0.906	1.99	0.490	0.498
	4a-5	14.68	1000	1.13	80.6	1.26	-0.20	0.879	1.86	0.458	0.442
p _i	4b-1	6.81	2037	1.13	53.1	2.45	-0.05	0.917	(2.98)	0.283	0.283
	4b-2	10.84	1959	1.13	27.1	2.65	-0.07	0.875	1.40	0.508	0.518
	4b-3	14.75	2123	1.13	31.0	3.02	-0.12	0.891	1.35	0.288	0.289

Note that quite recently, Delhaye et al. [5] have used the same MPI data as reference to validate some extrapolations from R12 void fraction data to water at high pressure, due to the high expense of such experiments.

3. New Heat Balance

To define the new heat balance, we are going to compare the axial profile of the mixture enthalpy h_m , Eq. (7), with that of the standard heat balance i.e., $q'z + h_{L,i}$. In [11], void fraction axial profile data is presented versus the measured relative enthalpy (or 'equilibrium' quality), Eq. (1). Previously to obtain h_m from data, we need to establish some basic assumptions about the thermodynamic properties used.

First, we neglect pressure drop, so assuming a constant pressure along the channel equal to the inlet pressure p_i . For the liquid enthalpy at subcooling, we assume the classic approach [1-2] of considering it practically equal to the ‘flow’ mixture enthalpy i.e., Eq. (1),

$$h_L \approx q'z + h_{L,i} \Rightarrow h_F = q'z_{sat} + h_{L,i} \Rightarrow z_{sat} = (h_F - h_{L,i})/q'. \quad (9)$$

So, the axial location of the saturation point z_{sat} can be readily calculated. The saturation properties of the liquid and vapor have been read in thermodynamic tables entering with inlet pressure, whereas the subcooled liquid properties have been obtained entering with the above calculated subcooled liquid enthalpy and the inlet pressure.

The actual axial distance z has been easily derived entering in Eq. (1) with the ‘equilibrium’ quality x_{eq} , extracted from the figures [11], and the applied heat flux reported. Finally, the local mixture density, Eq. (4), is calculated from the reported local cross-sectional average void fraction [11] and the above commented thermodynamic properties, and so the thermodynamic quality x_{th} , Eq. (3), which allows the calculation of $h_m(z)$, Eq. (7).

Figure 1a shows $h_m(z)$ for test 1-3, see Table 1, which is identical to tests 2a-3 and 4a-3. The circles represent the thermodynamic mixture enthalpy, Eq. (7), from the reduced data, the triangles the liquid enthalpy profile $h_L(z)$ and the fine line the standard heat balance $q'z + h_{L,i}$. The bold line is the simulation procedure followed in this work, which will be commented later.

Evidently, with the assumptions made, the mixture enthalpy along subcooling is greater than the subcooled liquid enthalpy. However, in reaching saturation the mixture enthalpy suffers such an abrupt reduction of its slope that it may be even below the standard heat balance. This dramatic change of slope of the mixture enthalpy would be clearly justified for the strong change suffered by the liquid enthalpy of a pure substance under heating, long time ago described by Thermodynamics, in passing from subcooled region, with growing values $h_L(z)$, to full saturated boiling, with a constant value h_F .

This behaviour of the mixture enthalpy $h_m(z)$ —rather different from the classic ‘flow’ enthalpy or standard heat balance i.e., $q'*z+h_{L,i}$ — has been definitely confirmed for the 24 tests in Table 1, see Figs. 2a-8a, and for the 31 ANL tests presented later in Table 2, see Figs. 15a-20a. Furthermore, this clear change of the mixture enthalpy slope in passing saturation has been also recently verified for some General Electric tests with low-pressure water [10]. Evidently, under uniform heat release along the channel, classic treatments cannot explain at all this marked, although physically justified, change of enthalpy slope.

The new suggested heat balance for flow boiling should respond to this change of slope. The authors have already suggested elsewhere [9-10] to explicitly include the slip ratio in the heat balance, see Eq. (8). Logically, this new included parameter should balance heat input with mixture enthalpy.

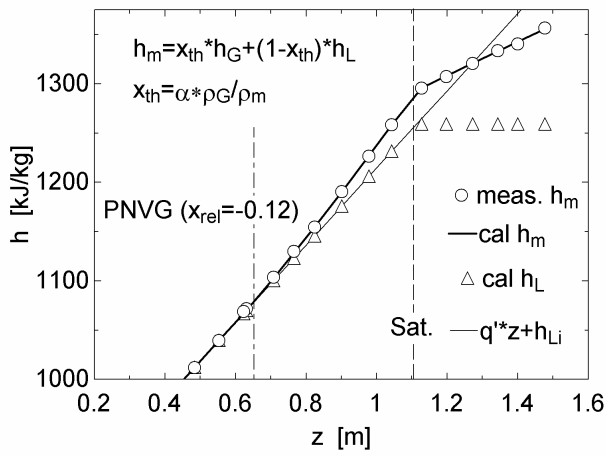


Fig.1a. Mixture enthalpy vs. z for Test 1-3.

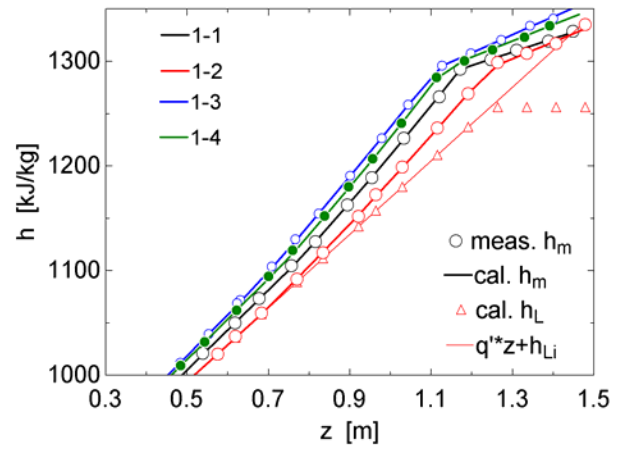


Fig.2a. Mixture enthalpy vs. z for group 1-Table 1.

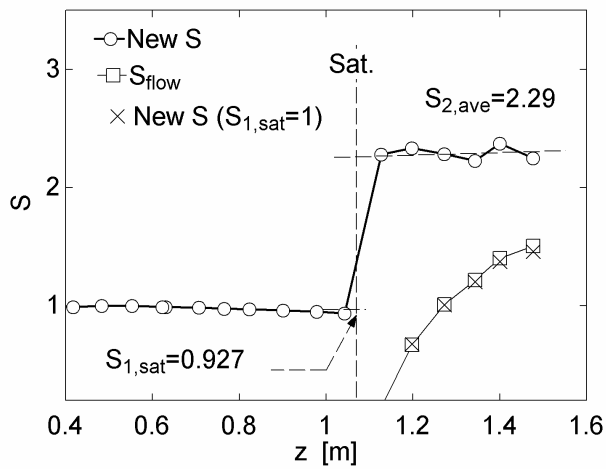


Fig. 1b. New slip ratio vs. z for test 1-3.

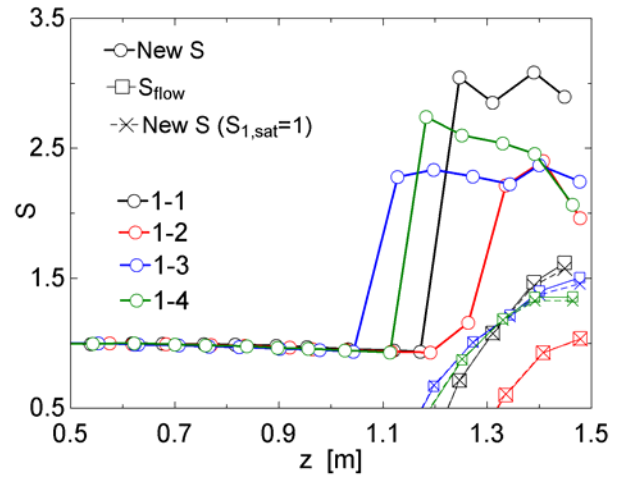


Fig. 2b. New slip ratio vs. z for group 1-Table 1.

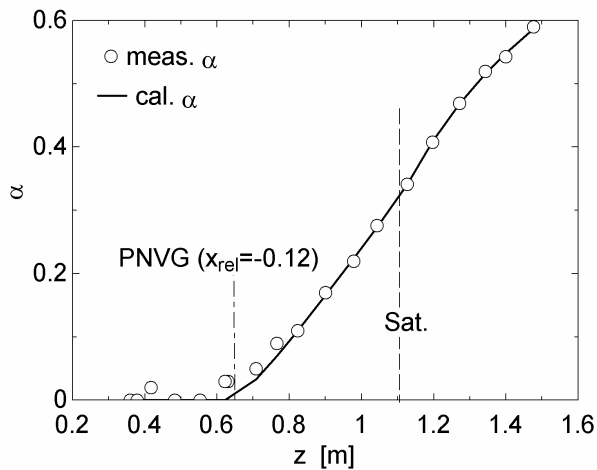


Fig. 1c. Void fraction vs. z for test 1-3.

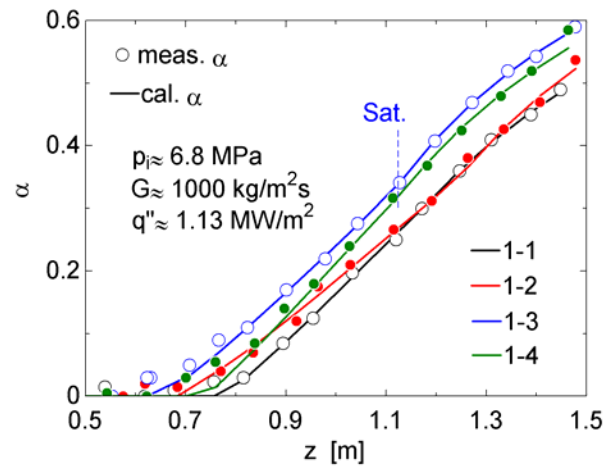


Fig. 2c. Void fraction vs. z for group 1-Table 1.

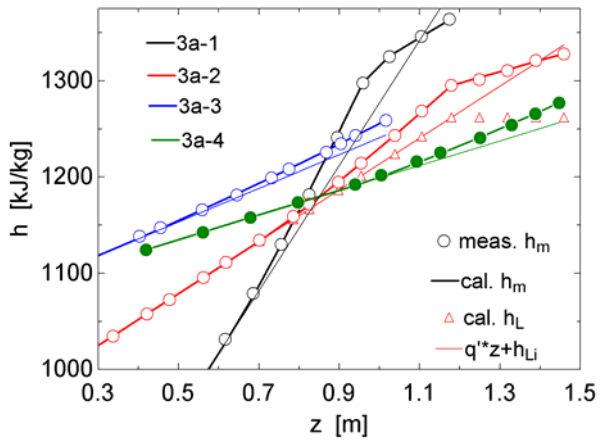


Fig. 5a. Mixture enthalpy vs. z for group 3a-Table 1.

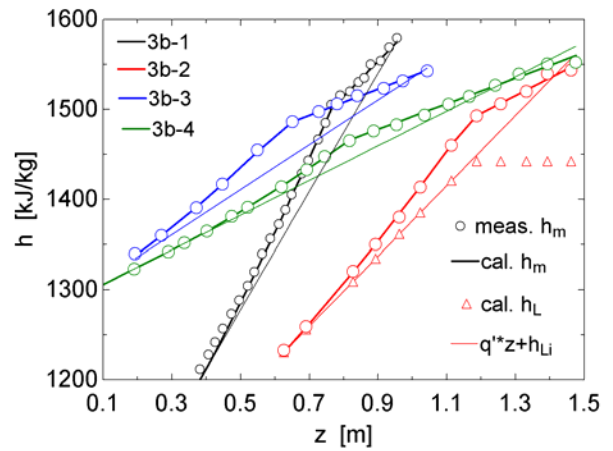


Fig. 6a. Mixture enthalpy vs. z for group 3b-Table 1.

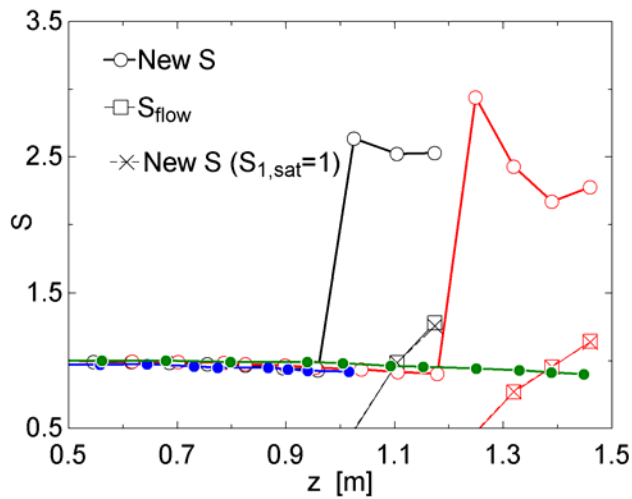


Fig. 5b. New slip ratio vs. z for group 3a-Table 1.

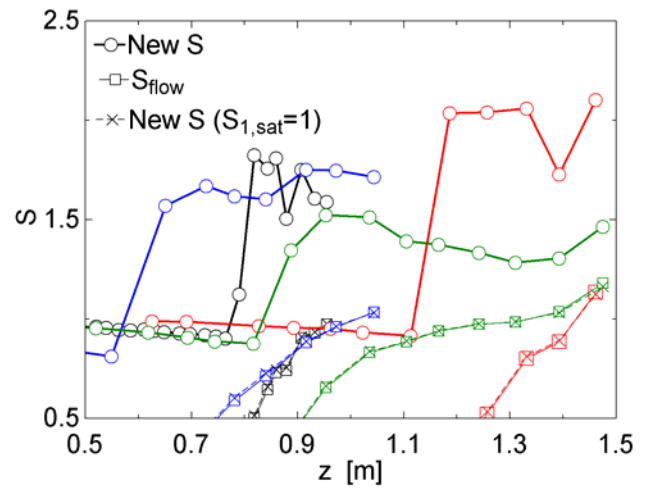


Fig. 6b. New slip ratio vs. z for group 3b-Table 1.

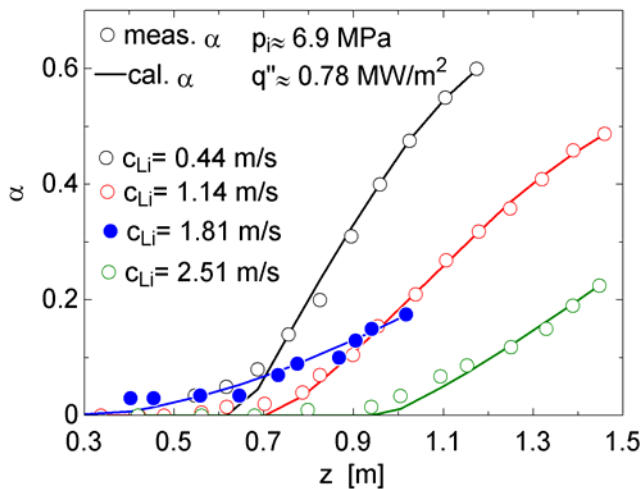


Fig. 5a. Void fraction vs. z for group 3a-Table 1.

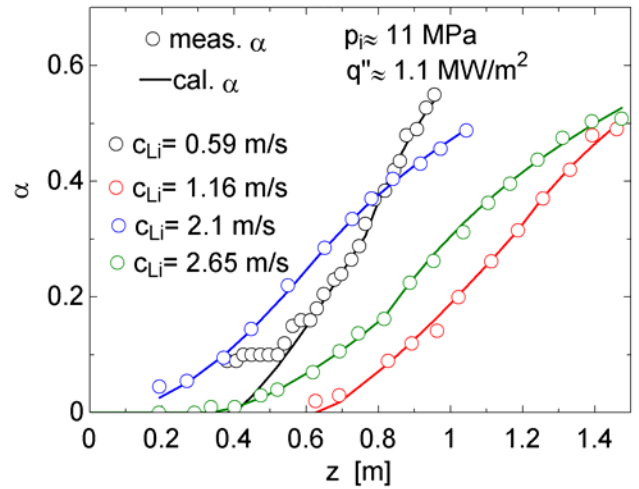


Fig. 6b. Void fraction vs. z for group 3b-Table 1

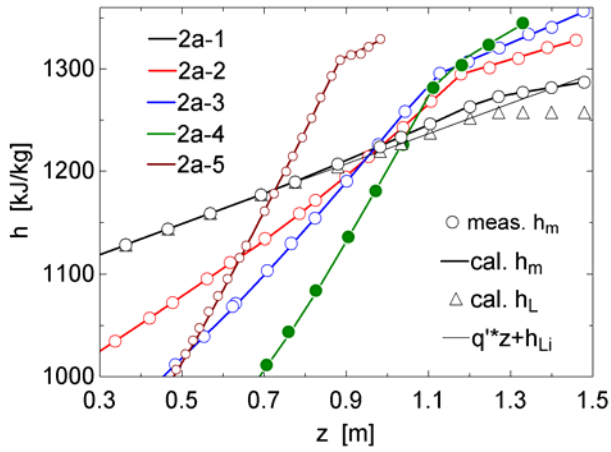


Fig. 3a. Mixture enthalpy vs. z for group 2a-Table 1.

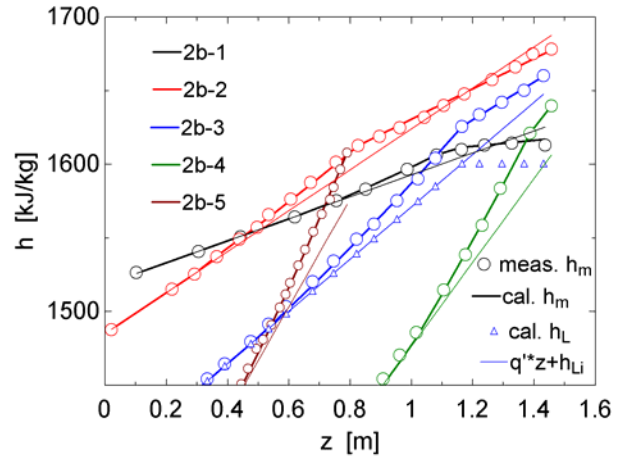


Fig. 4a. Mixture enthalpy vs. z for group 2b-Table 1.

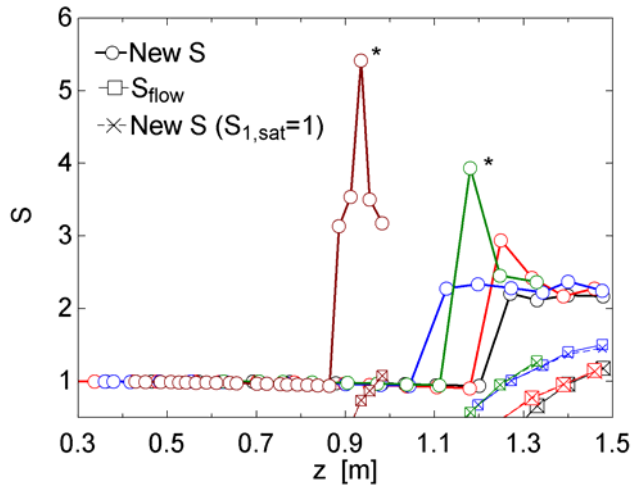


Fig. 3b. New slip ratio vs. z for group 2a-Table 1.

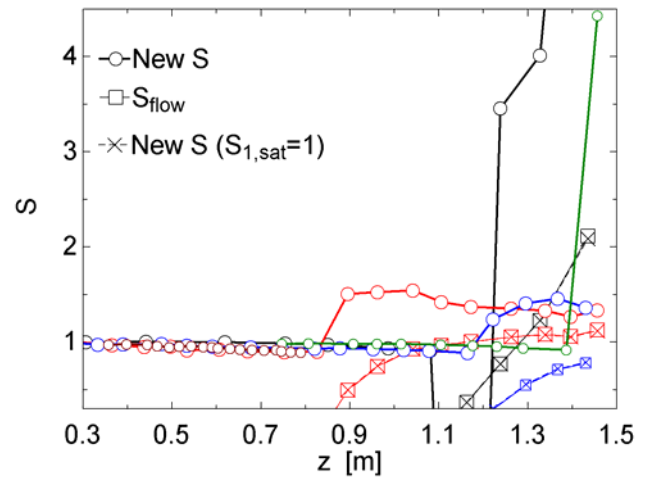


Fig. 4b. New slip ratio vs. z for group 2b-Table 1.

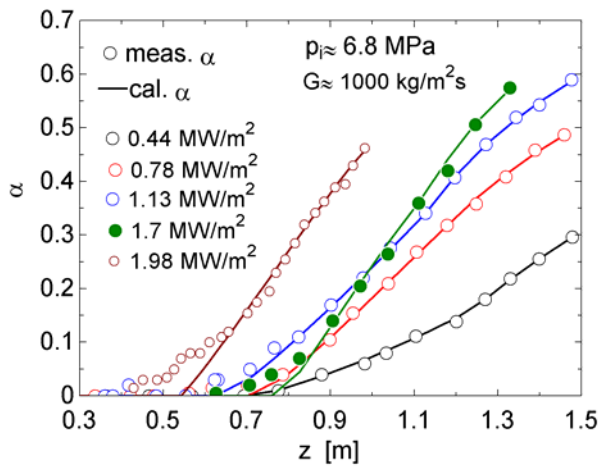


Fig. 3c. Void fraction vs. z for group 2a-Table 1.

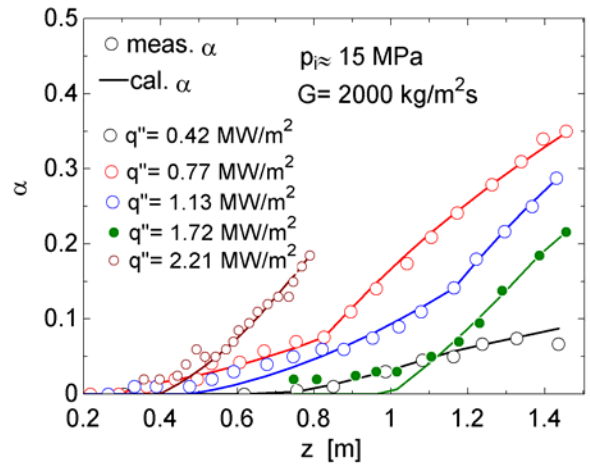


Fig. 4c. Void fraction vs. z for group 2b-Table 1.

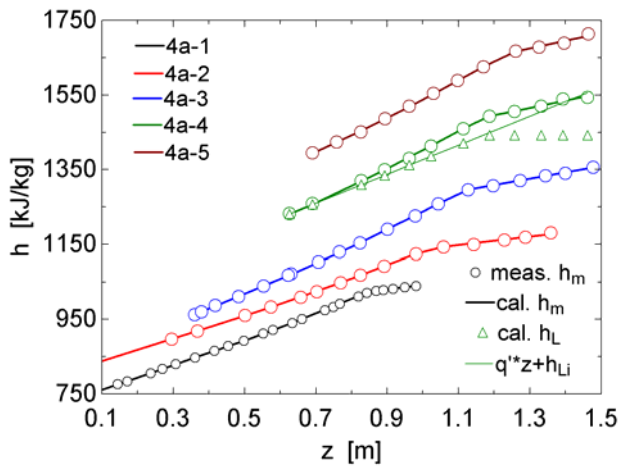


Fig. 7a. Mixture enthalpy vs. z for group 4a-Table 1.

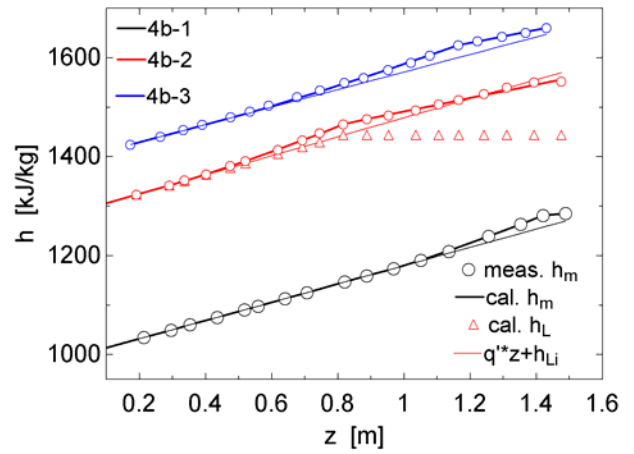


Fig. 8a. Mixture enthalpy vs. z for group 4b-Table 1.

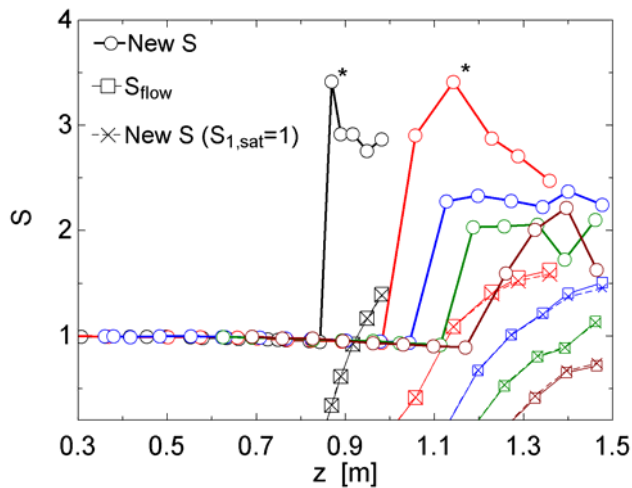


Fig. 7b. New slip ratio vs. z for group 4a-Table 1.

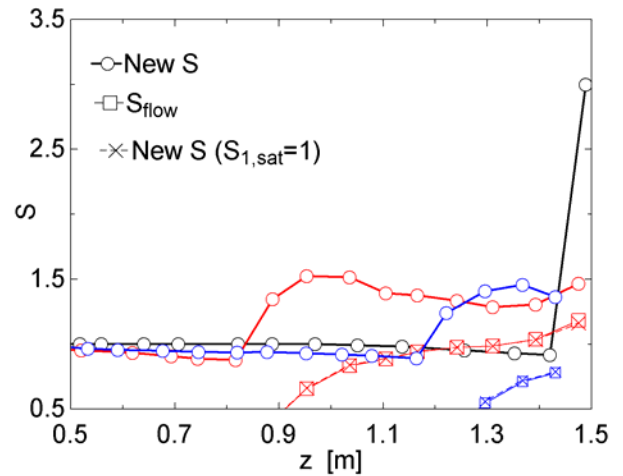


Fig. 8b. New slip ratio vs. z for group 4b-Table 1.

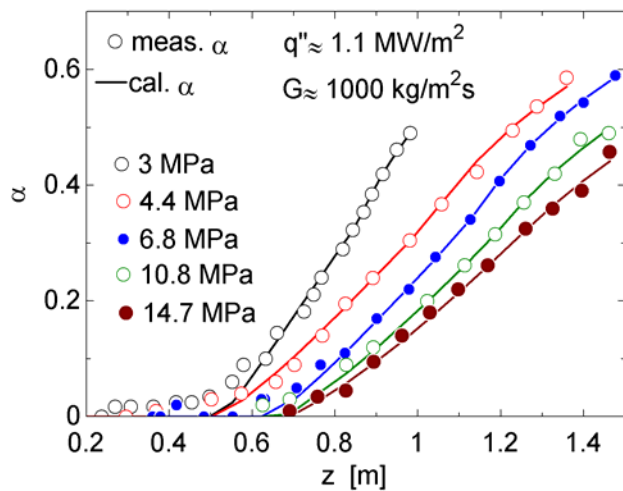


Fig. 7c. Void fraction vs. z for group 4a-Table 1.

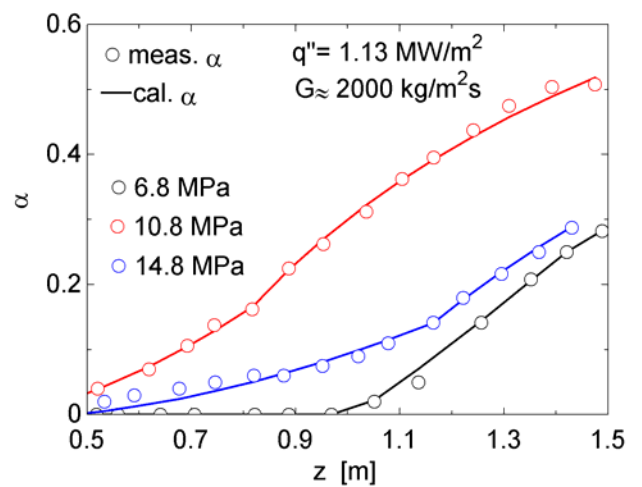


Fig. 8c. Void fraction vs. z for group 4b-Table 1.

However, the clear change of slope between subcooling and saturated boiling would suggest using two different slip ratios namely, S_1 for the subcooled zone, just until the saturation point, and S_2 for the full boiling region. Then, at subcooling, the new heat balance would be

$$h_m = q'z/S_1 + h_{L,i} \Rightarrow S_1 = q'z/(h_m - h_{L,i}). \quad (10)$$

After saturation, the evolution of the mixture enthalpy should be a continuation of the former one

$$h_m = q'(z - z_{sat})/S_2 + h_{m,sat} \Rightarrow S_2 = q'(z - z_{sat})/(h_m - h_{m,sat}). \quad (11)$$

Then, in Eq. (11), the mixture enthalpy at saturation, at the end of subcooling, is derived from Eq. (10), also including Eq. (9),

$$h_{m,sat} = q'z_{sat}/S_{1,sat} + h_{L,i} = (h_F - h_{L,i})/S_{1,sat} + h_{L,i}. \quad (12)$$

Now, substituting Eq. (12) in Eq. (11), we obtain

$$S_2 = [q'z - (h_F - h_{L,i})]/[h_m - h_{L,i} - (h_F - h_{L,i})/S_{1,sat}]. \quad (13)$$

Finally, by convenience, we derive an approximation to S_2 , Eq. (13), assuming that $S_{1,sat} \approx 1$

$$S_2(S_{1,sat} \approx 1) = [q'z - (h_F - h_{L,i})]/(h_m - h_F). \quad (14)$$

4. New Slip Ratio

Figure 1b presents the axial profile of S_1 —along subcooling, and S_2 —along full boiling, Eq. (10) and Eq. (13), respectively for test 1-3. Starting at one i.e., single flow, S_1 goes down smoothly until reaching saturation $S_{1,sat} = 0.927$. Evidently, as this slip ratio is less than one, the mixture enthalpy can be greater than the standard one, see Eq. (10). This new slip ratio cannot take negative values, and its order of magnitude, slightly less than one, would be confirmed by historic photographic measurements of vapor bubble velocity at subcooling [1-2].

After saturation, the new suggested slip ratio S_2 , Eq. (11), is clearly greater than one, although now, at difference from S_1 , its axial profile seems to be practically horizontal i.e., S_2 would be practically constant along saturated boiling. This would justify taking a constant value for the saturation region equal to the arithmetic average of their calculated values. As we can see in Figs.2c-8c, the good predictions of the void fraction in this region would also support this average. Alos, see later Figs. 15c-20c, which correspond to ANL void fraction predictions.

To check that this new parameter S_2 is effectively a slip ratio, we have compared the classic 'flow' slip ratio S_{flow} , Eq. (2), with an approximation to S_2 i.e., Eq. (14), in which we have

assumed that $S_{1,sat} \approx 1$ along saturation. We have plotted them starting at saturation because S_{flow} would take negative values at subcooling with the classic procedure, see Eq. (4).

As can be seen in Fig. 1b, the coincidence between them is very strong. Also highlight that the slight change from $S_{1,sat} = 0.927$ to $S_{1,sat} \approx 1$ means a completely different profile along saturation. The behaviour of the new slip ratio and the comparison between the classic slip ratio and such approximation to the new one can be seen in Figs. 2b-8b for the 24 tests in Table 1. Also, see later Figs. 15b-20b for the 31 ANL tests of Table 2.

Finally, note that the authors have recently verified elsewhere [9] the Equation (8), the new suggested heat balance, finding a quite strong relation between the classic slip ratio and the heat-mixture enthalpy ratio, although there for saturated flow boiling, which entered in the heated channel exactly as saturated liquid without vapor, i.e., $S_{1,sat} \approx 1$.

5. Void Fraction Prediction

The new procedure suggested here for calculating void fraction needs for values of S_1 and S_2 . As we have commented above, we will take a constant value for S_2 . However, for S_1 , we will assume a simple linear decay from $S_1=1$ at the starting point of boiling until saturation $S_1 = S_{1,sat}$ i.e.,

$$S_1 \approx 1 + (S_{1,sat} - 1)(z - z_{PNVG}) / (z_{sat} - z_{PNVG}), \quad (16)$$

where the axial position of the beginning of boiling or point of net vapor generation (PNVG) [13-14] has been denoted by z_{PNVG} .

By the sake of convenience, instead of directly searching the axial distance z_{PNVG} , first it has been searched the corresponding relative enthalpy value, denoted by $x_{eq-PNVG}$ in Table 1, which better fitted the void fraction in the subcooled region. Then the derivation of z_{PNVG} , necessary for Eq. (16), is immediate entering in Eq. (1) with $x_{eq-PNVG}$.

Now we are able of reproducing the heat balance i.e, the axial profile of the thermodynamic mixture enthalpy, provided we have the right two slip ratios i.e., $S_{1,sat}$ and $S_{2,ave}$, and the location of the point of net vapor generation or $x_{eq-PNVG}$. So, the bold line in Fig.1a is the simulated axial profile of such mixture enthalpy. Then, from the definition of h_m , Eq. (7), we can calculate the thermodynamic quality x_{th} and, finally, from Eq. (6), the void fraction is finally derived.

Figure 1c compares the measured axial profile of the void fraction with the calculated one following this new procedure for test 1-3 in Table 1. The model fails in the first region of subcooling, with very low values of the void fraction. Although for the second region i.e., fully developed subcooled boiling, and the full saturation zone the agreement is quite acceptable.

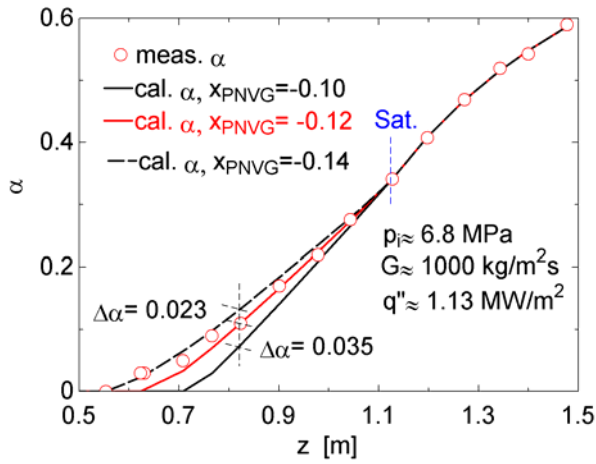


Fig. 9. Void fraction sensitivity to x_{PNVG} . Test 1-3, Table 1.

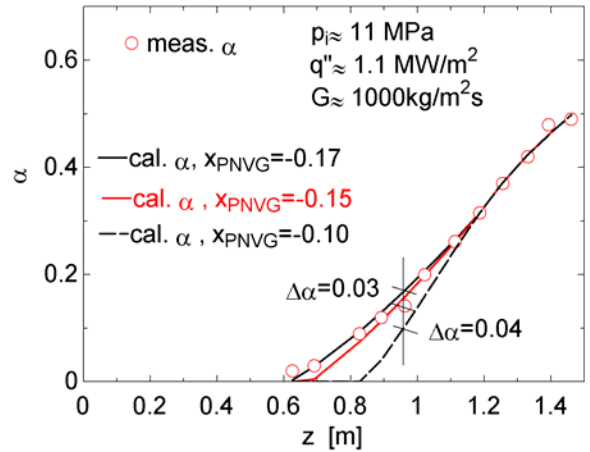


Fig. 12. Void fraction sensitivity to x_{PNVG} . Test 3b-2 Table 1.

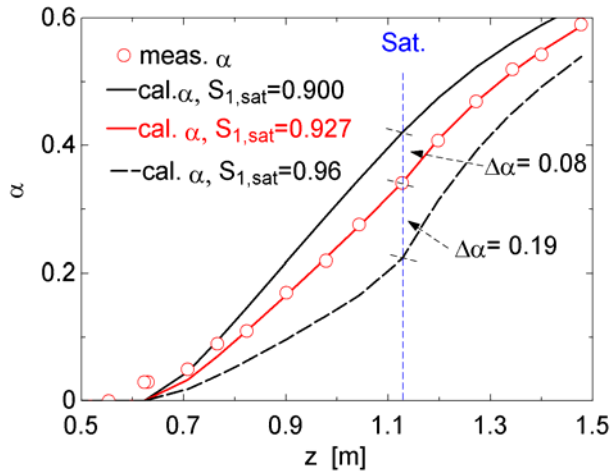


Fig. 10. Void fraction sensitivity to $S_{1,sat}$. Test 1-3, Table 1.

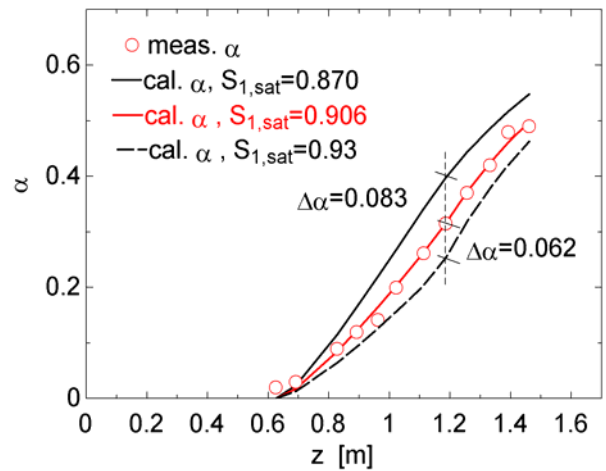


Fig. 13. Void fraction sensitivity to $S_{1,sat}$. Test 3b-2, Table 1.

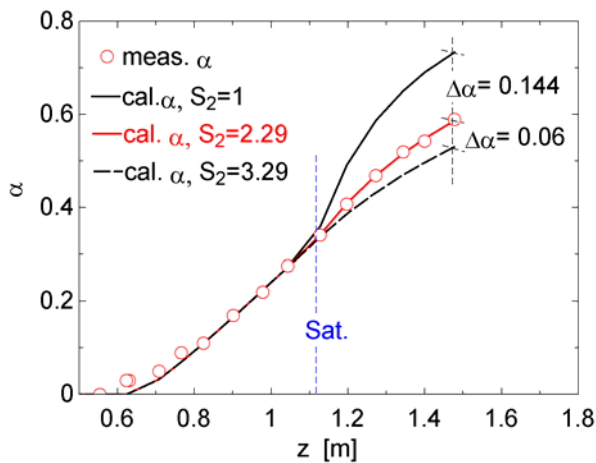


Fig. 11. Void fraction sensitivity to S_2 . Test 1-3, Table 1.

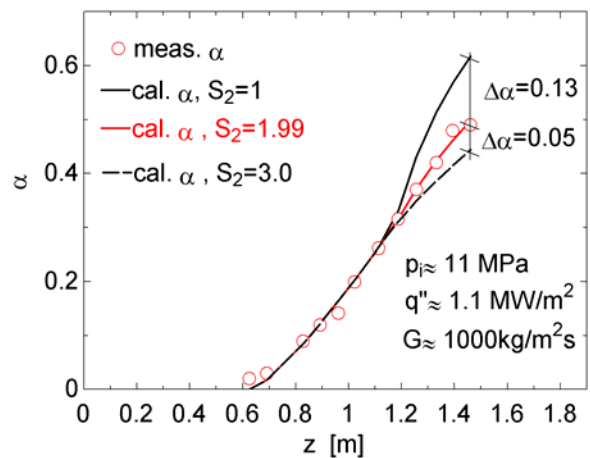


Fig. 14. Void fraction sensitivity to S_2 . Test 3b-2, Table 1.

The comparison between the measured and calculated axial profiles of the void fraction for the MPI set of tests analyzed, see Table 1, can be found in Figs 2c-8c. The values of the two slip ratios and the point of net vapor generation that better fit the axial void fraction profile data are shown in Table 1. Finally, Figs. 9-14 show some sensitivity analysis of the void fraction calculation to variations on the new slip ratios and the PNVG.

6. ANL Measurements of the Axial Profile of Void fraction

Many accurate measurements of the axial profile of the void fraction in the region of boiling with subcooling for water at medium pressure (1.12-4.23 MPa) and low subcooling were carried out in the sixties at the Argonne National Laboratory (ANL) for a wide range of severe operating conditions. The data were taken for natural and forced circulation in $12.7 \cdot 10^{-3}$ – $6.35 \cdot 10^{-3}$ m (0.5–0.25 inches) by $50.8 \cdot 10^{-3}$ m (2 inches) by 1.524 m (60 inches) rectangular channels over a velocity range of 0.305-1.83 m/s, and a ‘flow’ quality range of 0 to 6 %. Marchaterre et al. reported in [12] some representative runs to analyze the main trends about the influence of heat flux, mass velocity and pressure on void fraction.

Table 2. Conditions of some of the tests presented by Marchaterre et al. in [12]

# Test	p_i (MPa)	G (kg/m ² s)	q'' (MW/m ²)	$\Delta T_{sub,i}$ (° C)	$c_{L,i}$ (m/s)	$x_{eq-PNVG}$	$S_{1,sat}$ (* ave)	$S_{2,ave}$	$\alpha_{o,mea}$	$\alpha_{o,cal}$
236	1.12	406	0.12	5.4	0.46	-0.006	0.916*	3.21	0.600	0.626
234	1.12	527	0.12	4.1	0.59	-0.006	0.900*	2.88	0.570	0.591
231	1.13	674	0.12	3.2	0.76	-0.005	0.900*	2.55	0.545	0.557
230	1.13	733	0.12	5.4	0.83	-0.004	0.885*	2.40	0.550	0.552
228	1.12	380	0.15	7.3	0.43	-0.014	0.874	3.9	0.660	0.658
225	1.12	500	0.15	5.1	0.56	-0.010	0.890*	3.57	0.600	0.609
222	1.12	683	0.15	4.3	0.77	-0.008	0.868*	2.78	0.570	0.585
217	1.12	475	0.20	7.6	0.53	-0.012	0.896*	3.5	0.630	0.688
213	1.12	670	0.20	4.8	0.76	-0.008	0.850*	2.7	0.68	0.678
212	1.12	729	0.20	4.2	0.82	-0.008	0.845*	2.6	0.675	0.669
209	1.12	473	0.25	9.0	0.53	-0.013	0.889*	3.28	0.710	0.750
207	1.12	578	0.25	7.8	0.65	-0.013	0.896*	2.95	0.710	0.725
206	1.12	645	0.25	6.9	0.73	-0.013	0.862*	2.75	0.725	0.724
203	1.80	434	0.15	6.3	0.50	-0.014	0.895*	2.70	0.550	0.588
201	1.82	604	0.15	4.8	0.70	-0.011	0.845	2.60	0.515	0.525
247	1.81	789	0.15	3.3	0.92	-0.008	0.857*	2.50	0.480	0.469
199	1.81	417	0.20	8.6	0.48	-0.020	0.890	3.40	0.595	0.623
197	1.82	459	0.20	7.9	0.53	-0.017	0.865	3.30	0.640	0.614
189	1.81	621	0.20	5.8	0.72	-0.010	0.854*	2.95	0.560	0.567
193	1.82	377	0.25	13.4	0.43	-0.030	0.905	3.1	0.680	0.703
192	1.81	453	0.25	10.3	0.52	-0.020	0.870*	3.00	0.695	0.686
190	1.81	601	0.25	7.7	0.69	-0.015	0.865*	2.80	0.650	0.636
168	4.23	329	0.15	11.6	0.41	-0.030	0.895	3.00	0.390	0.401
167	4.23	404	0.15	8.9	0.50	-0.025	0.890	2.95	0.375	0.362
153	4.24	708	0.15	4.8	0.88	-0.012	0.859*	2.76	0.295	0.269
173	4.23	289	0.20	15.9	0.35	-0.030	0.915	3.5	0.480	0.476
172	4.23	362	0.20	12.7	0.45	-0.030	0.880	3.38	0.440	0.444
154	4.22	722	0.20	5.9	0.90	-0.012	0.872	2.84	0.350	0.322
187	4.23	380	0.25	14.0	0.47	-0.040	0.94	3.25	0.460	0.475
186	4.23	458	0.25	12.2	0.56	-0.030	0.905	3.16	0.420	0.446
183	4.23	743.8	0.25	7.6	0.92	-0.020	0.880	2.79	0.35	0.363

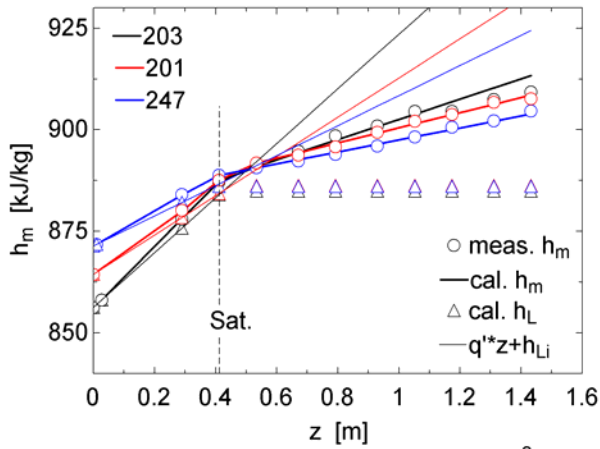


Fig. 17a. h_m vs. z . 1.82 MPa & 0.15 MW/m²-Table 2.

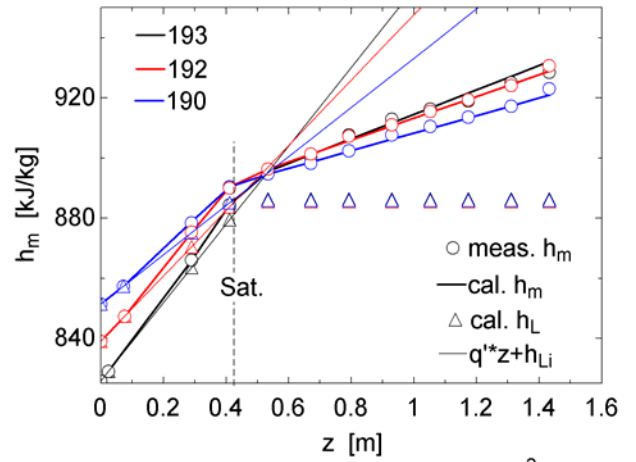


Fig. 18a. h_m vs. z . 1.82 MPa & 0.25 MW/m²-Table 2.

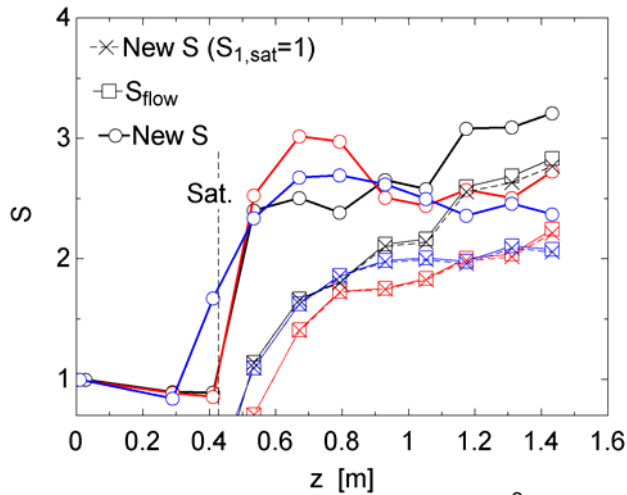


Fig. 17b. S vs. z . 1.82 MPa & 0.15 MW/m²-Table 2.

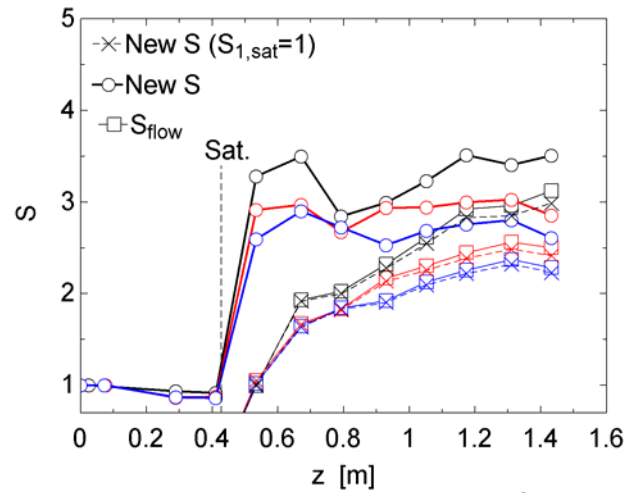


Fig. 18b. S vs. z . 1.82 MPa & 0.25 MW/m²-Table 2.

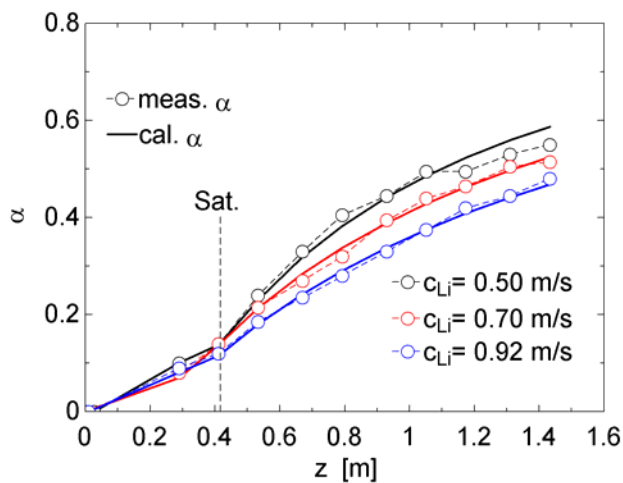


Fig. 17c. α vs. z . 1.82 MPa & 0.15 MW/m²-Table 2.

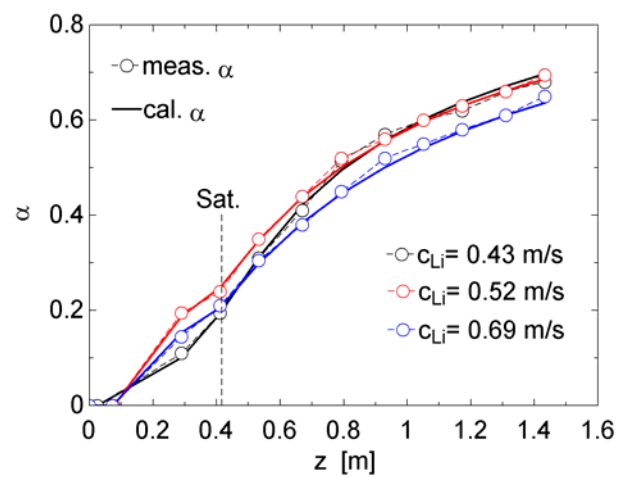


Fig. 18c. α vs. z . 1.82 MPa & 0.25 MW/m²-Table 2.

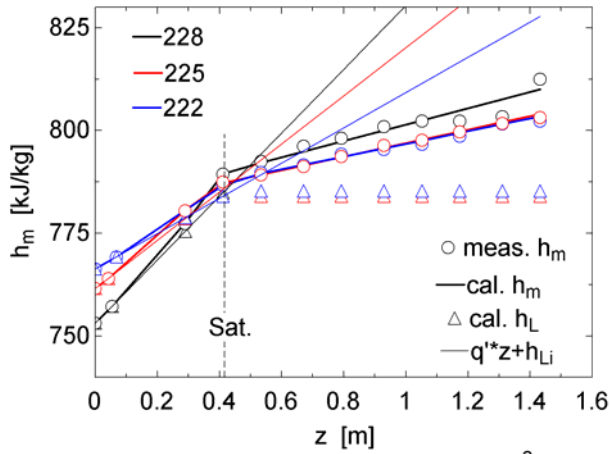


Fig. 15a. h_m vs. z . 1.12 MPa & 0.15 MW/m²-Table 2.

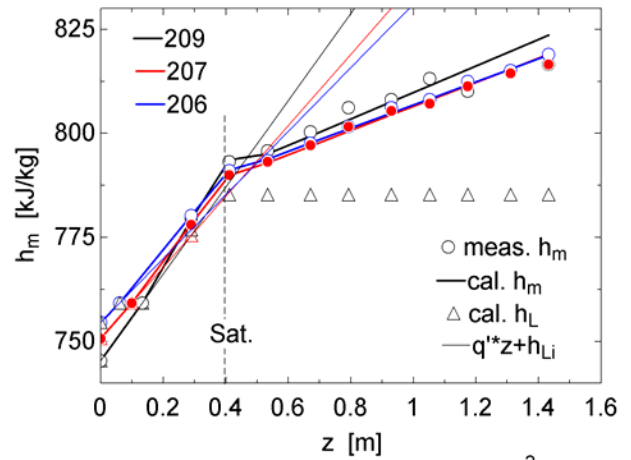


Fig. 16a. h_m vs. z . 1.12 MPa & 0.25 MW/m²-Table 2.

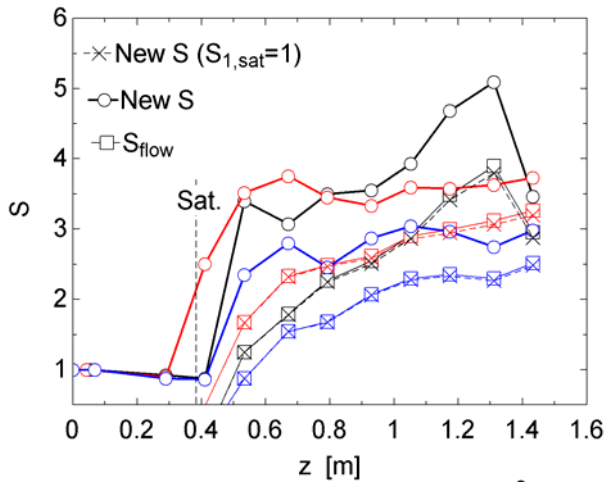


Fig. 15b. S vs. z . 1.12 MPa & 0.15 MW/m²-Table 2.

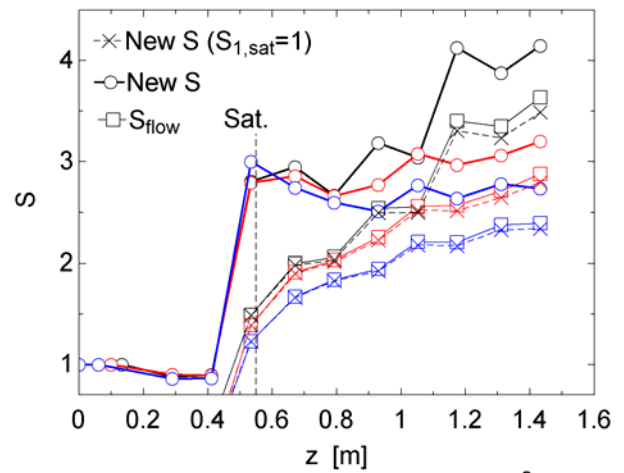


Fig. 16b. S vs. z . 1.12 MPa & 0.25 MW/m²-Table 2.

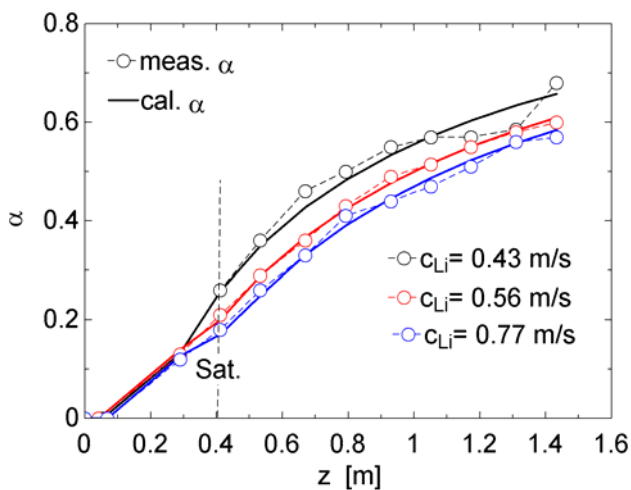


Fig. 15c. α vs. z . 1.12 MPa & 0.15 MW/m²-Table 2.

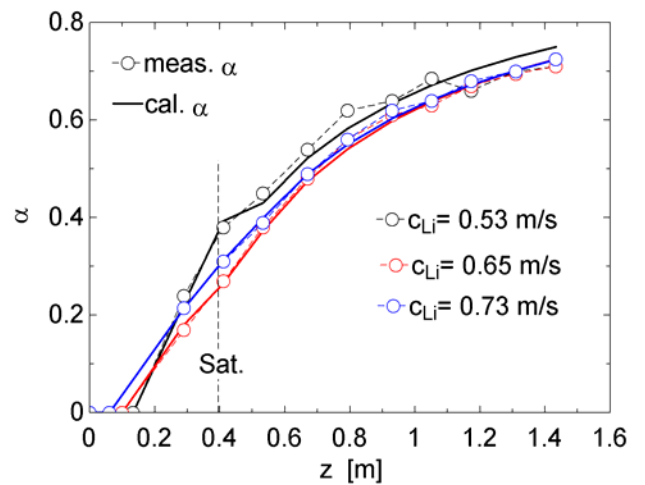


Fig. 16c. α vs. z . 1.12 MPa & 0.25 MW/m²-Table 2.

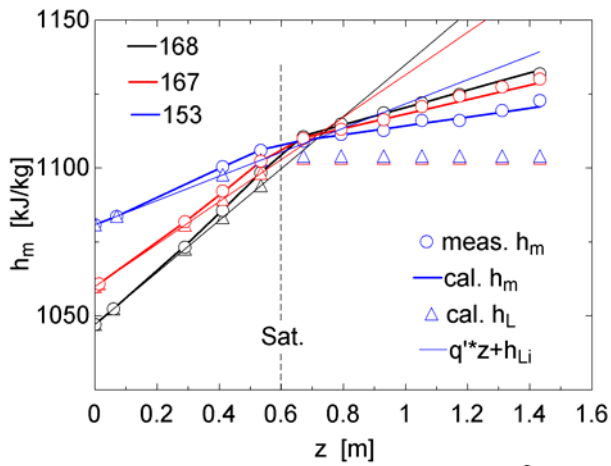


Fig. 19a. h_m vs. z . 4.23 MPa & 0.15 MW/m²-Table 2.

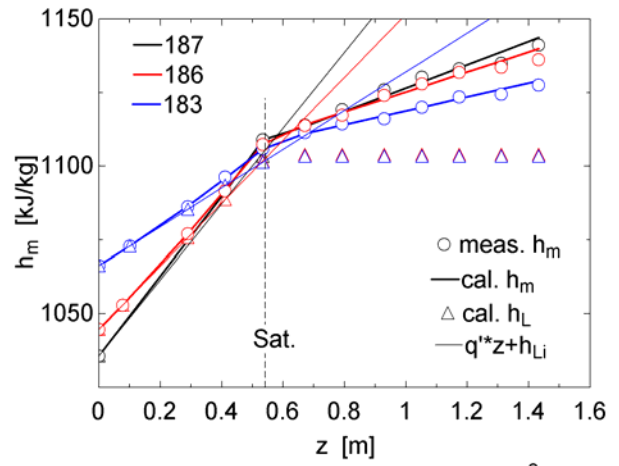


Fig. 20c. h_m vs. z . 4.23 MPa & 0.25 MW/m²-Table 2.

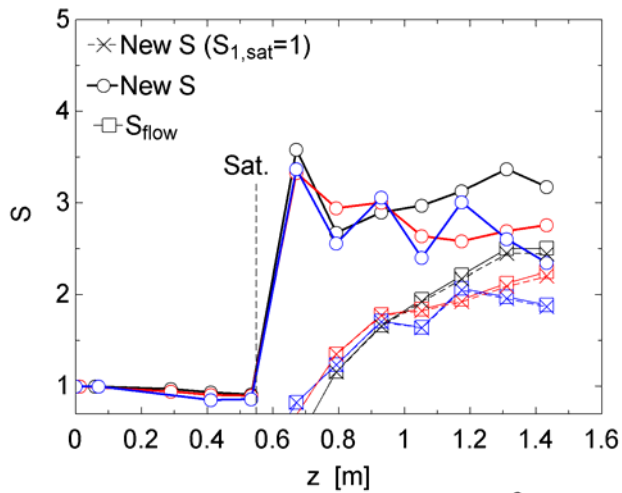


Fig. 19b. S vs. z . 4.23 MPa & 0.15 MW/m²-Table 2.

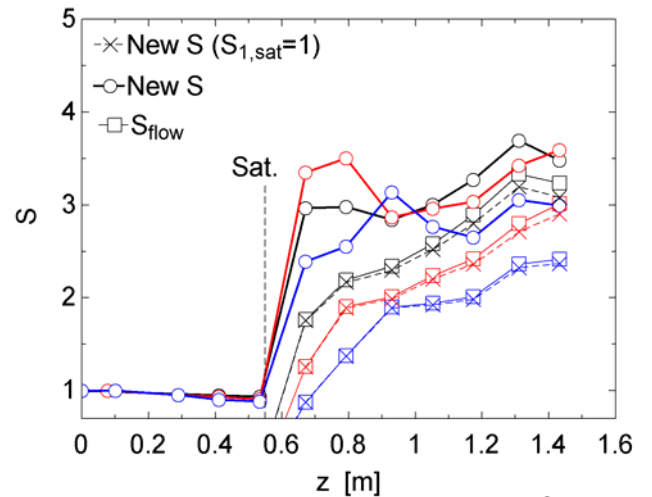


Fig. 20b. S vs. z . 4.23 MPa & 0.25 MW/m²-Table 2.

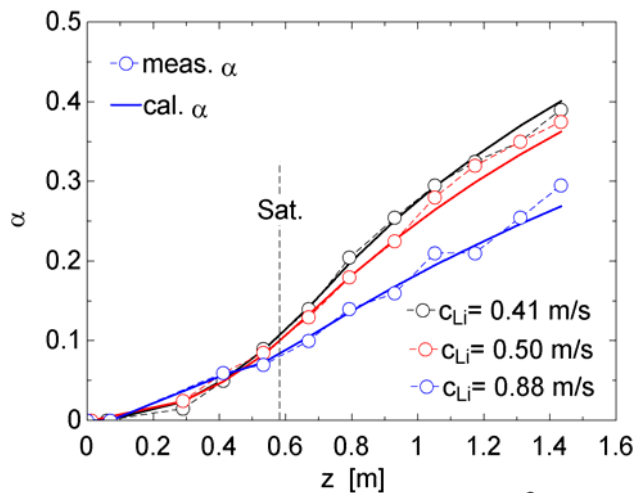


Fig. 19c. α vs. z . 4.23 MPa & 0.15 MW/m²-Table 2.

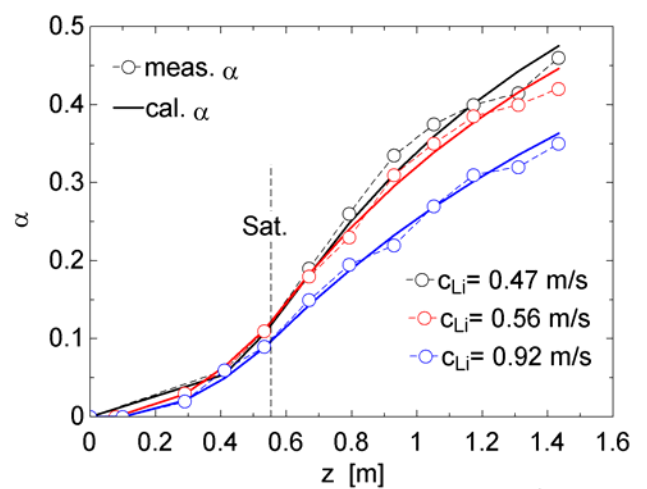


Fig. 20c. α vs. z . 4.23 MPa & 0.25 MW/m²-Table 2.

From the tests reported for the wider channel i.e., 12.7×10^{-3} m [12], we have selected, see Table 2, for the different pressures, 24 tests in which the inlet velocity was varied, but keeping constant the heat flux. The name of the tests is the same as reported by Marchaterre et al. [12]. So, at 1.12 MPa, Figs. 15-16 represent: a) the mixture enthalpy profile, b) the new slip ratio profile and c) the calculated and measured void fraction for two different heat fluxes. Figures 17-18 correspond to 1.83 MPa, and finally, Figs. 19-20 are for 4.23 MPa. The behaviour and trends of the new variables is identical to the MPI tests. So confirming the new heat balance.

7. Conclusions

The main novelty of this work about flow boiling is to use classic thermodynamic relationships between vapor weight and volumetric fractions i.e., to deal with the well-known thermodynamic quality.

So, we define a thermodynamic mixture enthalpy, which suffers a dramatic change of slope at saturation under uniform heat flux. In many vapor volumetric fraction data [11-12, 15], the axial profile of the measured void fraction also suffers a change of curvature at saturation.

In the new energetic expression proposed here, the absorbed heat is balanced with such thermodynamic mixture enthalpy through a new slip ratio, which is closely related to the classic 'flow' slip ratio. An intuitive explanation of this slip ratio inclusion could be the physical fact that the vapor bubbles velocity is different from the subcooled or saturated bulk liquid velocity. If we are treating simultaneously these two different velocities along the same distance i.e., the same control volume, their time scales should be also different. Therefore, the slip ratio would act as a scaling factor between two different time scales. Heat would enter into the control volume through the condensing vapor bubbles—as long as the heated wall is completely covered of bubbles [14], with a time scale different from the inlet bulk liquid.

With the new heat balance proposed here, the accurate calculation of the axial profile of the void fraction would be based on the prediction of three parameters namely, the point of net vapor generation (PNVG) expressed as an 'equilibrium' quality value, the new slip ratio just at saturation $S_{1,sat}$ (less than unity although close to it, 0.85-0.94) and an average value of the new slip ratio along full saturation S_2 (1.4-3.8 for the tests analyzed here).

There are strong experimental evidences of the constancy of the new slip ratio along full saturation S_2 . As more uniform S_2 is more regular the axial profile of void fraction is. Even for the tests in which S_2 suffers strong oscillations along the channel, the average value gives good approximations to the experimental void fraction data. Furthermore, the constancy of S_2 would be coherent with the fact that the heat is uniformly applied.

For some ANL tests at the lowest pressures and with very low subcooling, there are also indications of that S_1 is practically constant approaching saturation. In these tests—with asterisk in Table 2, we have used the average of S_1 values in the new heat balance instead of $S_{1,sat}$. This could be explained by the photographic studies of Griffith et al. [14]. So, at subcooling, the heated wall is partially bare, with the bubbles forming strands along the wall. Then S_1 would

decrease following the covering degree of wall by the bubbles. However, at the end of subcooling approaching saturation, the wall is completely covered with several layers of bubbles. In this last situation, the energy transferred to the liquid from the heated wall would be controlled by the bubbles, which are migrating from the wall for condensing into the bulk liquid i.e., the time scale difference between vapor and liquid would be fully established.

Partial sensitivity analysis with some MPI tests, see Figs. 9-14, show that a decrease of 0.03 in $S_{1,sat}$ could imply a calculated void fraction absolute difference with data of about 0.06-0.08; although an increase of 0.03 approaching to one i.e., to the classic heat balance, would mean about a 0.19 of absolute error. By the other side, an increase of 1.0 in S_2 would only provoke an absolute decrease of 0.05-0.06. Furthermore, it has been checked that with $S_2=1$ i.e., using the classic heat balance at full boiling region, the void fraction calculated exhibit a difference of about 0.13-0.15 with data. In conclusion, classic heat balance cannot explain at all the measured void fraction.

Finally, it would seem that the sensitivity of void fraction calculation at subcooling is not very high to some variations of the point of net vapor generation (PNVG). So, reductions or increases of such point by 0.02 would mean about 0.02-0.04 of net difference with data at fully developed subcooled region.

About the dependence of the new slip ratio parameters with the main operational parameters namely, inlet pressure, heat flux and inlet velocity, it would be clear, from Table 1 and 2, a logic and very clear dependence of $S_{1,sat}$ and S_2 on the liquid inlet velocity $c_{L,i}$. So, higher the inlet velocity is lower both new slip ratios are. About pressure, Fig. 7b would show that S_2 diminishes with increasing pressure.

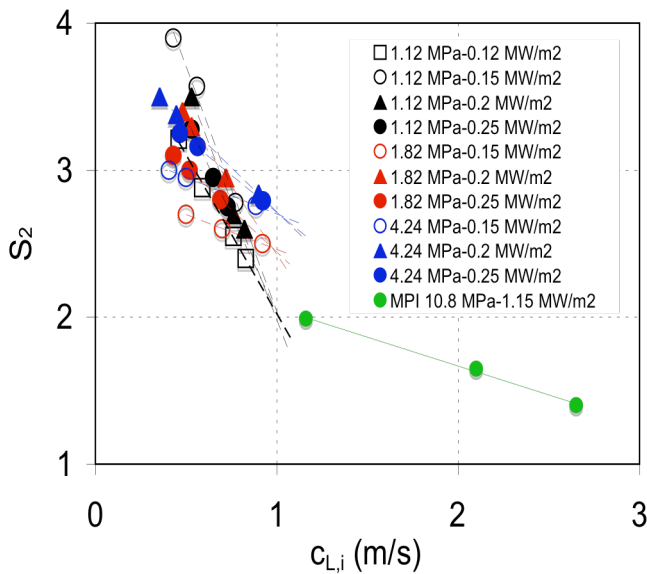


Fig. 21. S_2 vs. Inlet liquid velocity. ANL tests.

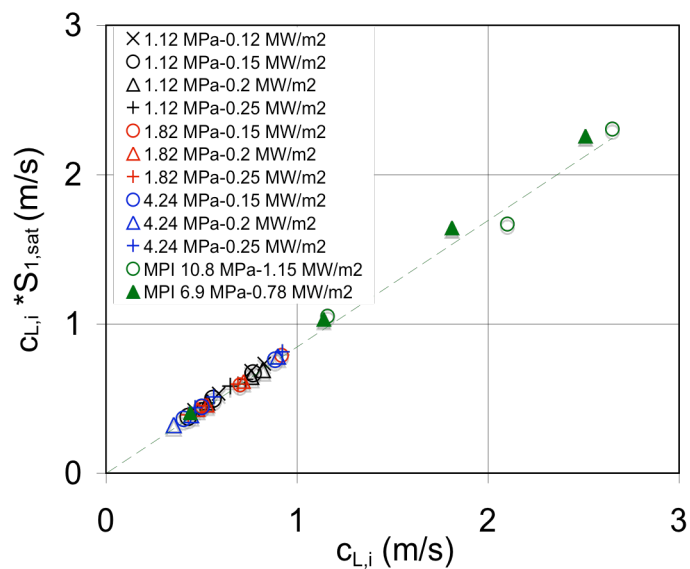


Fig. 22. $S_{1,sat}$ vs. Inlet liquid velocity. ANL tests.

About heat flux, the trends of the new slip ratios are not so clear. Then, as a first approximation to the prediction of the new slip ratios in function of the main operational parameters, we have represented S_2 in function of the inlet velocity for different pressures and heat fluxes, see Fig. 21; whereas, based on previous works [9], we have plotted $c_{Li} * S_{1,sat}$ versus c_{Li} , see Fig. 22. Watching such linear plots, it seems possible to accurately fit these key parameters. Work is in progress.

Acknowledgements

The authors want to thank to the Spanish Minister of Education and Science (MEC) the funding of this research through the research project DPI2005-08654-C04-04.

References

- [1] Collier JG. Nuclear steam generators and waste heat boilers. In Kakaç S. Boilers, evaporators and condensers. New York: John Wiley and Sons, 1991: Chapter 9.
- [2] Collier JG, Thome JR. Convective boiling and condensation, (3rd edition). Oxford, UK: Oxford University Press, 1994.
- [3] Lahey RT Jr, Moody, FJ. The thermal hydraulics of a boiling water nuclear reactor. La Grange Park: American Nuclear Society, 1979.
- [4] Levy S. Forced convection subcooled boiling-prediction of vapor volumetric fraction. *International Journal of Heat and Mass Transfer*. 1967;19:99-113.
- [5] Delhaye JM, Maugin F, Ochterbeck JM. Void fraction predictions in forced convective subcooled boiling of water between 10 and 18 MPa. *International Journal of Heat and Mass Transfer*. 2004;47:4415-4425.
- [6] Zuber N, Findlay JA. Average volumetric concentration in two phase flow systems. *ASME Journal of Heat Transfer*. 1965;87:453-467.
- [7] Bilicki Z, Michaelides EE. Thermodynamic nonequilibrium in liquid-vapour flows. *Journal of Non-Equilibrium Thermodynamics*. 1997;22:99-109.
- [8] Bilicki Z, Giot M, Kwidzinski R. Fundamentals of two-phase flow by the method of irreversible thermodynamics. *International Journal of Multiphase Flow*. 2002;28:1983-2005.
- [9] Collado, FJ, Monné C, Pascau A, Fuster D, Medrano A. Thermodynamics of void fraction in saturated flow boiling. *Journal of Heat Transfer-Transactions of ASME*. 2006;128:611-615.
- [10] Collado, FJ, Monné C, Pascau A. Changes of enthalpy slope in subcooled flow boiling. *Heat and Mass Transfer*. 2006; 42: 437-448.
- [11] Bartolomei GG, Brantov VG, Molochnikov YuS, Kharitonov YuV, Solodkii VA, Batashova, GN, Mikhailov VN. An experimental investigation of true volumetric vapour content with subcooled boiling in tubes. *Thermal Engineering*. 1982;29:132-135.
- [12] Marchaterre JF, Petrick M, Lottes PA, Weatherhead RJ, Flinn WS. Natural and forced-circulation boiling studies. Chicago: Argonne National Laboratory, ANL-5735, 1960.
- [13] Saha P, Zuber N. Point of net vapor generation and vapor void fraction in subcooled boiling. Tokyo: Proceedings of The Fifth International Heat Transfer Conference, 1974: paper B4.7.
- [14] Griffith P, Clark JA, Rohsenow, WM. Void volumes in subcooled boiling systems. New York: ASME paper 58-HT-19, 1958.
- [15] Ahmad, SY. Axial distribution of bulk temperature and void fraction in a heated channel with inlet subcooling. *Journal of Heat Transfer-Transactions of ASME*. 1970;595-609.